Food Chemistry: X 23 (2024) 101636

Contents lists available at ScienceDirect

Food Chemistry: X

journal homepage: www.sciencedirect.com/journal/food-chemistry-x

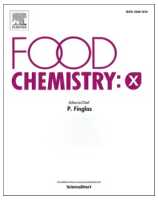

Effect of stigmasterol and polyglycerol polyricinoleate concentrations on the preparation and properties of rapeseed oil-based gel emulsions

Wenjie Xie [a], Caili Tang [a], Yu Zhang [a], Wei Fan [a], Jingping Qin [a], Hang Xiao [b], Shiyin Guo [a,*], Zhonghai Tang [a,*]

[a] College of Food Science and Technology, Hunan Engineering Technology Research Center for Rapeseed Oil Nutrition Health and Deep Development, Hunan Agricultural University, Changsha 410128, China
[b] Department of Food Science, University of Massachusetts, Amherst, MA 01003, USA

ARTICLE INFO

Keywords:
Gel emulsion
Polyglycerol polyricinoleate
Rapeseed oil
Stigmasterol
Network structure

ABSTRACT

Emulsion gels mimic the rheological properties of solid and semi-solid fats, offering a viable solution to replace conventional fats in low-fat food formulations. In this study, gel emulsions stabilized with stigmasterol (ST) and polyglycerol polyricinoleate (PGPR) complexes were prepared. Initially, we examined the effect of the ST/PGPR complex on the mechanism of gel emulsion stabilization. Our findings revealed that the gel emulsion formulated with 3% PGPR and ST exhibited a robust structure, effectively stabilizing the entire system and ensuring uniform distribution, and increasing ST concentration led to greater stability of the gel emulsion system. Stability assessments demonstrated that gel emulsions containing 3% PGPR and varying ST concentrations exhibited remarkable thermal stability and effectively delayed oil oxidation. These results underscore the high stability of gel emulsions stabilized with the ST/PGPR complex, highlighting their potential as a margarine substitute.

1. Introduction

Emulsion gel, filled with emulsion droplets, possesses robust mechanical properties and distinctive functional characteristics owing to its gel mesh structure, making it extensively utilized in the food industry (Poyato, Astiasarán, Barriuso, & Ansorena, 2015). According to current research, tropical vegetable fats and animal fats often produce large amounts of saturated fatty acids, and even trans-fatty acids (Cui, Guo, & Meng, 2023). Excessive intake of saturated and trans-fatty acids can increase the risk of cardiovascular and cerebrovascular diseases and metabolic syndromes, greatly endangering human health (Cui et al., 2023). Emulsion gels with rheological properties similar to those of solid and semi-solid fats provide a novel solution for the construction of non-hydrogenated, zero-trans, and low-saturated fatty acid solid fats to replace conventional fats and develop low-fat foods (Cui et al., 2023). Moreover, Emulsion gels exhibit a delicate, resilient texture and a three-dimensional network that safeguards flavor compounds and pigments (Zhi et al., 2023). Consequently, they find widespread applications in the food and pharmaceutical industries (Poyato et al., 2015; Zhong et al., 2020). Due to these properties, emulsion gels are primarily used in the food industry for two main applications: as fat substitutes in meat products and as delivery systems for food nutrients (Lin, Kelly, & Miao, 2020). Thus, this is a promising technology for the development of nutritious and healthy foods.

Emulsion gels, also known as emulgels or gelled emulsions (Dickinson, 2012), consist of two-phase systems where one phase is dispersed into the other (Sereti, Kotsiou, Biliaderis, Moschakis, & Lazaridou, 2023). Emulsion gels are thermodynamically unstable; therefore, amphiphilic polymers are required to improve the stability of emulsion gels (Wang et al., 2020). While current research predominantly focuses on oil droplets stabilized by proteins or surfactants (Lin, Liang, Zhong, Ye, & Singh, 2021), the escalating global population raises concerns about potential protein shortages (Bascuas, Morell, Hernando, & Quiles, 2021). Thus, there is a growing need for alternative emulsifiers. As a member of the sterol family, stigmasterol (ST), a natural 6–6–6-5 tetracyclic sterol (Kaur, Chaudhary, Jain, & Kishore, 2011), is widely present in vegetable oils such as soybean, peanut, and sunflower oils (Liu, Ma, Xia, Guo, & Zeng, 2022). ST exhibits various biological activities including antioxidant, anti-inflammatory, and antitumor properties (Gao, Maloney, Dedkova, & Hecht, 2008; Navarro, De Las

* Corresponding authors at: College of Food Science and Technology, Hunan Agricultural University, Changsha 410128, China.
E-mail addresses: weifan@hunau.edu.cn (W. Fan), qinjingping@hunau.edu.cn (J. Qin), hangxiao@umass.edu (H. Xiao), gsy@hunau.edu.cn (S. Guo), tangzh@hunau.edu.cn (Z. Tang).

https://doi.org/10.1016/j.fochx.2024.101636
Received 14 March 2024; Received in revised form 29 May 2024; Accepted 6 July 2024

Heras, & Villar, 2001; Wang et al., 2017). ST possesses an amphiphilic structure with a large oleophilic surface and polar OH head group (Tang et al., 2022), contributing to its significant hydrophobicity (Tao, Shkumatov, Alexander, Ason, & Zhou, 2019). Based on the results of preliminary experiments, a mixture of ST and rapeseed oil, along with a certain proportion of the aqueous phase, can be processed into gel-like water-in-oil (W/O) emulsions using high-speed shearing. ST can reduce the surface tension of W/O gel emulsions and form a rigid interfacial layer on the surface of emulsion droplets (Cercaci, Rodriguez-Estrada, Lercker, & Decker, 2007). However, it is common practice to utilize ST in isolation to stabilize emulsions, and little is known about how mixtures of various emulsifiers influence the structure and stability of emulsions. In contrast to low-fat emulsions, W/O gel emulsions are typically stabilized using various forms of emulsifiers (Bai, Huan, Rojas, & McClements, 2021; Ge et al., 2017). Polyglycerol polyricinoleate (PGPR) is an effective food emulsifier composed of a polyglycerol headgroup esterified with one or more polyricinoleate chains (Price, Gray, Watson, Vieira, & Wolf, 2022). Its excellent emulsifying properties are attributed to the excellent water-binding capacity of its long hydrophilic polyglycerol chain (Márquez, Medrano, Panizzolo, & Wagner, 2010). Rapeseed oil, being the second most abundant oil globally and boasting excellent nutritional qualities (Chew, 2020; Yang et al., 2022), was selected as the primary oil base for our emulsion gel.

In this study, we investigated the combined effects of ST and PGPR on the properties of W/O-type gel emulsions to prepare a healthier fat substitute. The formation mechanisms of rapeseed oil-based W/O-type gel emulsions, as well as their impacts on emulsion droplet size and stability, were analyzed via polarized light microscopy, laser confocal microscopy, and X-ray diffraction (XRD). Additionally, we examined the influence of ST and PGPR concentrations on the rheological properties, thermodynamic properties, and stability of these gel emulsions. To the best of our knowledge, this is the first time that ST and PGPR have been used as co-stabilizers for W/O-type gel emulsions, which has significant implications for the development and use of ST and PGPR in the food, pharmaceutical, and cosmetic industries. We believe that this study could enhance and expand the application of gel emulsions as promising fat substitutes.

2. Materials and methods

2.1. Materials

ST (90%) was supplied by Source Leaf Biotechnology (Shanghai, China), and commercial-grade rapeseed oil was purchased from a local supermarket. All other chemicals and reagents utilized in this experiment were of analytical grade.

2.2. Methods

2.2.1. Preparation of gel emulsion

To determine the critical water phase, 5 g rapeseed oil was combined with 6% (w/w) ST and a mixture of 2% (w/w) PGPR, followed by deposition in a water bath under thermostatic magnetic stirring until complete dissolution. Preheated deionized water at 50 °C was gradually added to the system, comprising water phases of 5, 15, 25, 35, 45, 55, 65, 75, and 85% of the total mass fraction of the system. Using an Ultra Turrax homogenizer (IKA Ultra Turrax digital, Model T18 basics, Germany) with a 180 mm head, the samples were homogenized at 13,000 rpm for 3–4 min. After homogenization, the samples were stored for 24 h at 4 °C (±2 °C). Three samples were prepared for each condition.

To determine the critical ST concentration, 5 g rapeseed oil was mixed with complexes of 2% (w/w) PGPR and varying concentrations of ST (3%, 4%, 5%, 6%, 7%, and 8% of the oil weight, w/w). The mixture underwent dissolution in a water bath under thermostatic magnetic stirring, followed by gradual addition of preheated deionized water at 50 °C, constituting 65% of the total mass. Homogenization was performed using an Ultra Turrax T18 homogenizer at 13,000 rpm for 3–4 min, and samples were stored at 4 °C (±2 °C) for 24 h before analysis. Three samples were prepared for each condition.

To determine the joint effects of PGPR and ST concentrations on gel emulsion, 5 g rapeseed oil with 2%, 3%, and 6% (w/w) PGPR, along with varying concentrations of ST (4%, 5%, 6%, 7%, and 8%, w/w) were used. Following dissolution in a water bath under thermostatic magnetic stirring, preheated deionized water at 50 °C was added, constituting 65% of the total mass. Homogenization was achieved using an Ultra Turrax T18 homogenizer at 13,000 rpm for 3–4 min, and samples were stored at 4 °C (±2 °C) for 24 h before analysis. Three samples were prepared for each condition.

2.2.2. Microstructure analysis

The microstructures of the gel emulsions were observed at 25 °C using a polarizing microscope (CX31; Olympus, Tokyo, Japan). A suitable amount of gel emulsion was placed on a glass slide and covered with another glass slide to ensure an even distribution of the sample. The droplet shape and arrangement in the gel emulsion were observed under the non-polarized light mode, whereas the distribution of ST and PGPR crystals in the system was visualized in the same area using the polarized light mode (Chen, Bian, Cao, Shi, & Meng, 2023). All images were captured at a magnification of 500 x.

Fluorescence micrographs of the gel emulsions were obtained via laser confocal microscopy (CLSM). The oil phase of the gel emulsion was stained with Nile Red at a concentration of 0.01 wt%. The structural morphology of the gel emulsion was inspected using excitation/emission wavelengths of 488/515 nm for Nile Red (Liu et al., 2023). All fluorescence images were obtained using a 63× objective lens in an inverted configuration.

2.2.3. Average particle size analysis

The diameters of the gel emulsion droplets in the images captured by the microscope were measured using OLYCIA m3 Software (Shanghai Puhe Photoelectric Technology Co., Ltd., Shanghai, China). The average surface area of the particles ($d_{3,2}$) was calculated using the following formula:

$$d_{3,2} = \frac{\sum n_i d_i^3}{\sum n_i d_i^2} \quad (1)$$

where n_i represents the number of droplets with diameter d_i (Zhang et al., 2022).

2.2.4. XRD analysis

XRD spectroscopy (Shimadzu, Kyoto, Japan) employing reflection geometry and Cu Kα radiation (λ = 1.542 Å) at 40 kV and 30 mA, respectively, was utilized to analyze the crystallization patterns of the gel emulsion, according to a previously described method (Tang et al., 2022). Measurements were taken between 5° and 50° (2θ), with a step size of 0.02°. The diffractograms were analyzed using MDI Jade 6.0 software (Materials Data Ltd., Livermore, CA, USA).

2.2.5. Rheological property analysis

The rheological properties of the gel emulsions were analyzed using a Kinexus Pro Advanced Rheometer (Malvern Instruments Ltd., Malvern, UK), according to a previously described method (Tang et al., 2022). A stainless-steel cone plate geometry (40 mm, 1° angle, and 1 mm truncation) was selected. Specifically, frequency sweep (0.1–100 Hz) experiments were performed under constant strain within the linear viscoelastic domain. The temperature sweep (25–100 °C) tests were carried out at a constant frequency of 1 Hz and a heating rate of 2 °C/min. The apparent viscosity (0.01 s^{-1} to 100 s^{-1}) was measured with a constant shear strain. Thixotropy recovery sweep tests were conducted with a gap distance of 1 mm, shear strain of 0.01%, fixed frequency of 1 Hz, and shear rate ranging from 0.1 s^{-1} to 10 s^{-1} and then returning to

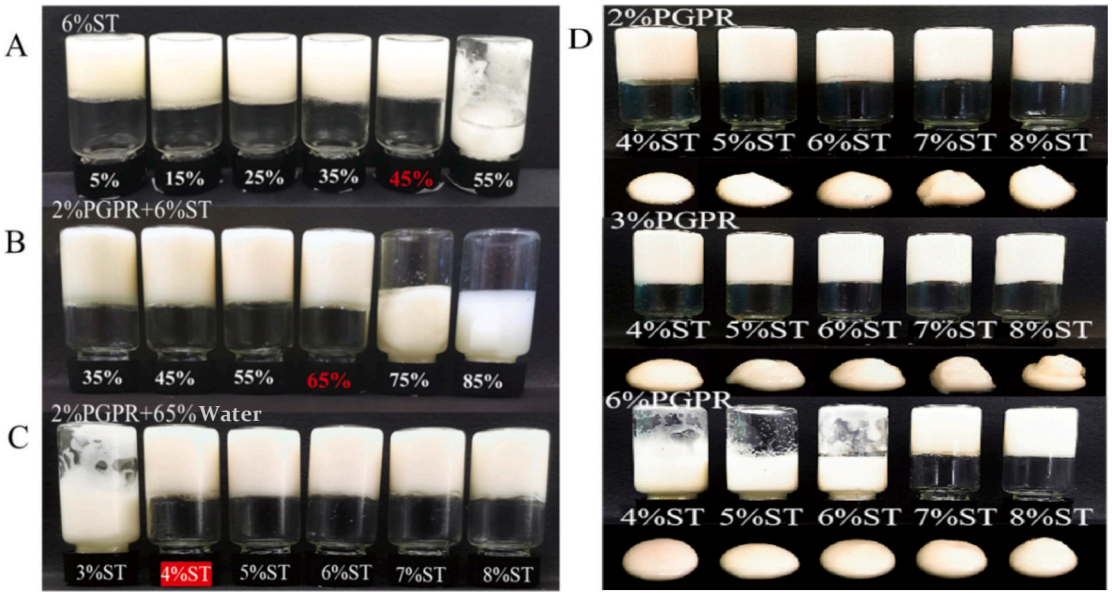

Fig. 1. (A) Appearance of various aqueous gel emulsions at 6% stigmasterol (ST) concentration with different aqueous solutions (5%, 15%, 25%, 35%, 45%, and 55%); (B) Appearance of various gel emulsions at 2% PGPR and 6% ST with different aqueous solutions (35%, 45%, 55%, 65%, 75%, and 85%); (C) Appearance of various gel emulsions with different ST concentrations at 2% PGPR and 65% water; (D) Appearance of various gel emulsions with different concentrations of PGPR and ST (Aqueous solution concentrations of all samples constant to be 65%).

0.1 s^{-1}. Each shearing rate lasted 5 min. The viscosity of the gel emulsion after the initial shearing stage is represented as n1, whereas the viscosity after the third shearing stage is denoted as n2. The viscosity recovery value was calculated as n2/n1. All experiments were performed at 25 °C, except for the temperature sweep tests.

2.2.6. Thermodynamic analysis

The thermodynamic behaviors of ST and the gel emulsion were determined using a DSC3 differential scanning calorimeter (Mettler Toledo, Port Melbourne, Australia). Approximately 1 mg of ST and 50 mg of the gel emulsion were placed in separate aluminum pans, with an empty aluminum pan used as a reference. The temperature was increased from 25 °C to 200 °C at a heating rate of 5 °C/min, and the thermodynamic changes were recorded using the instrument software.

2.2.7. Stability analysis

2.2.7.1. Physical stability. To test the storage stability, 5 g gel emulsion was placed in a 10 mL glass serum bottle and stored at room temperature for 30 d. The physical stability was evaluated by observing the appearance and measuring the average surface area of the emulsion gel droplets.

To test the heat stability, a suitable amount of gel emulsion was placed in a 10 mL glass serum bottle and stored in an oven at 50 °C, 60 °C, and 70 °C for 24 h. Heat stability was evaluated by observing the appearance and measuring the average surface area of the emulsion gel droplets.

2.2.7.2. Oxidative stability. Accelerated oxidation experiments were conducted according to the recommended AOCS method (Brühl, 1997). Gel emulsion samples, prepared with PGPR complexes at concentrations of 2%, 3%, and 6% of the oil weight (w/w), along with varying concentrations (w/w) of ST, were contained in glass serum bottles. Fresh gel emulsion samples and those subjected to storage in an oven at 60 °C for 5 d were used to determine lipid peroxides. It is noteworthy that a storage time of 1 d at 60 °C is equivalent to 30 d of storage at 20 °C based on the Arrhenius equation (Wang, Li, Liu, & Tong, 2022). The determination of peroxide value followed the method outlined in ISO 27107 (2008), "Animal and vegetable fats and oils – determination of peroxide value-potentiometric end-point determination."

2.2.8. Statistical data analysis

All tests were performed in triplicate. Data were presented as mean ± standard deviation. SPSS 20 software (SPSS Inc., Chicago, IL, USA) was used to analyze the variance of the experimental data, with a significance level of $p < 0.05$. Data were visualized using Origin 2018 software (OriginLab Corporation, Northampton, MA, USA).

3. Results and discussion

3.1. Appearance analysis

Using high-speed shear homogenization, we investigated the impact of the aqueous-phase mass fraction (5–85 wt% of the total sample system), ST, and PGPR concentration on the formation of rapeseed oil-based gel emulsions. Fig. 1A indicates that when ST served as the primary emulsifier, a maximum of 45 wt% water phase was achieved with 6% ST. This may be because of the low viscosity of the 6% ST-prepared gel emulsion, resulting in carrying less water phase (≤45 wt%). Typically, emulsifiers are added to reduce the interfacial tension (Choi, Decker, & McClements, 2009), generating gel emulsions with high viscosity and stability. Fig. 1B demonstrates that when 2% PGPR was introduced as an emulsifier, the system could accommodate a maximum water phase of 65% with 6% ST. This suggests that incorporating PGPR enhances the formation ability of the gel emulsion system when combined with ST in the external phase, enabling it to carry more water. Fig. 1C showcases a stable gel emulsion with 2% PGPR and 65% water. Moreover, as the ST concentration increased, the gel emulsion displayed a more pronounced gel-like structure.

To improve the structure and viscosity of the external phase of the gel emulsion and increase its stability, the effects of PGPR and ST concentrations on the gel emulsion at a water-phase ratio of 65 wt% were further studied. As depicted in Fig. 1D, the gel emulsion in the 65% water phase exhibited a smoother texture and more uniform appearance as the ST concentration increased. During high-speed shear, gel emulsions were prepared with 2% and 3% PGPR and ST. Gel emulsions were only produced when the ST concentration exceeded 6% with 6% PGPR.

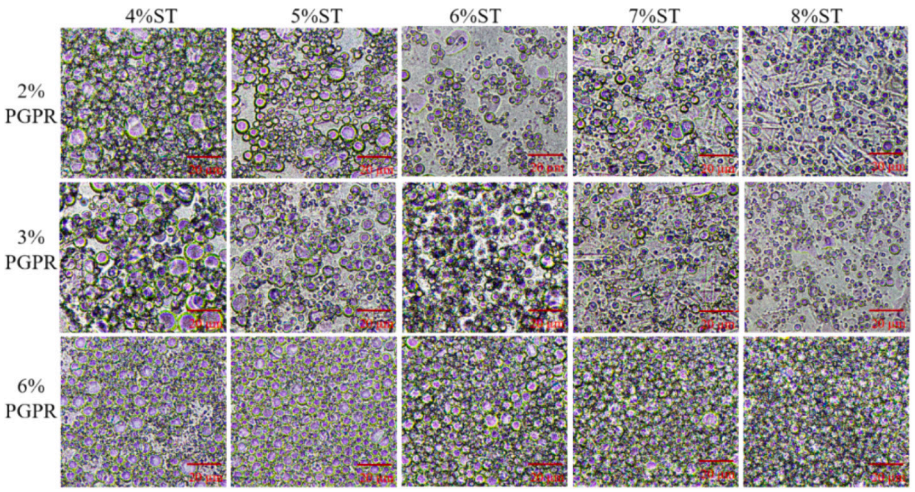

Fig. 2. Microscopic images of gel emulsions prepared with 2%, 3%, and 6% PGPR and various ST concentrations under ordinary light (Aqueous solution concentrations of all samples constant to be 65%). Scale bar = 20 μm.

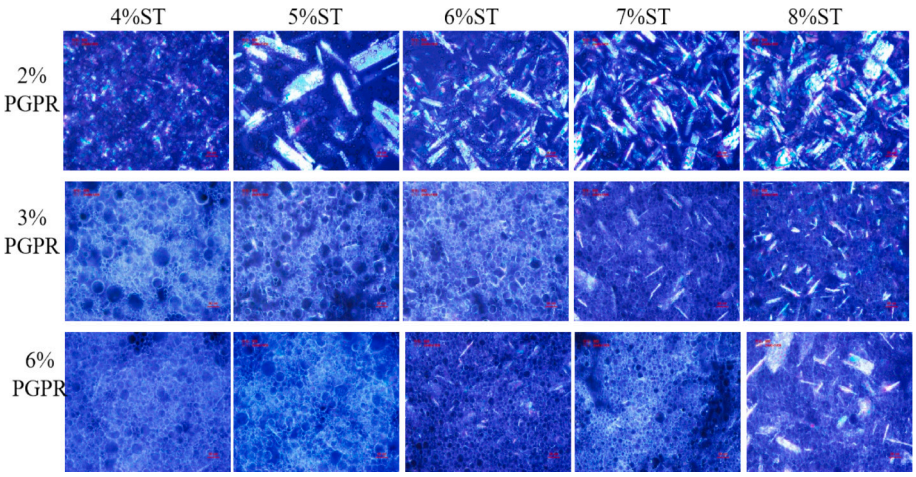

Fig. 3. Microscopic images illustrating gel emulsions prepared with 2%, 3%, and 6% PGPR and different ST concentrations under polarized light (Aqueous solution concentrations of all samples constant to be 65%). Scale bar = 20 μm.

This enhancement in emulsification efficacy at higher PGPR concentrations may lead to a predominantly emulsified system owing to reduced viscoelasticity (Okuro, Gomes, Costa, Adame, & Cunha, 2019). Initial visual analysis indicated that ST and emulsifier concentrations influenced gel emulsion formation, with higher PGPR and lower ST concentrations making it more challenging to achieve a gel emulsion. Based on our observations, it appears that PGPR and ST can exhibit both synergistic and competitive behavior, depending on their specific concentrations.

At lower concentrations (e.g., 2% PGPR and 4% ST), we observed a synergistic effect, where the combination enabled the formation of gel emulsions with higher water content (65 wt%) compared to using ST alone (45 wt% water with 6% ST). However, at higher PGPR concentrations (e.g., 6% PGPR), a higher ST concentration (at least 7%) was required to stabilize the gel emulsion with 65 wt% water, suggesting a competitive interaction. These observations indicate that the interplay between PGPR and ST is complex and likely depends on factors such as their relative concentrations and the overall emulsion composition. Consequently, we further investigated PGPR and ST concentrations based on microscopic structure, rheological properties, and gel emulsion stability.

3.2. Optical microstructure analysis

As depicted in Fig. 2, optical microstructure analysis revealed that the prepared rapeseed oil-based gel emulsions contained relatively small droplets. As the ST concentration increased, these emulsion gel droplets underwent shrinkage and exhibited more uniform dispersion throughout the gel emulsion. The distribution of droplets within the gel emulsion altered with varying PGPR concentrations. Specifically, at 2% PGPR, emulsion droplets exhibited a random distribution. At 3% PGPR, droplet distribution became uniform, whereas at 6% PGPR, emulsion gel droplets appeared more compact. This could be attributed to the high surface activity of PGPR at higher concentrations, which aggregated neighboring droplets in the emulsion (Mao, Calligaries, Barba, & Miao, 2014), resulting in a more concentrated droplet distribution. Based on these findings, it is plausible to assume that ST and PGPR concentrations affect the microstructure of the gel emulsion.

3.3. Polarized light microstructure analysis

Polarized light microscopy (Fig. 3) also revealed that the number of rod-shaped crystals in the gel emulsion system increased dramatically as the ST content increased, and their distribution became more concentrated. The number of white crystalline rings in the gel emulsion system

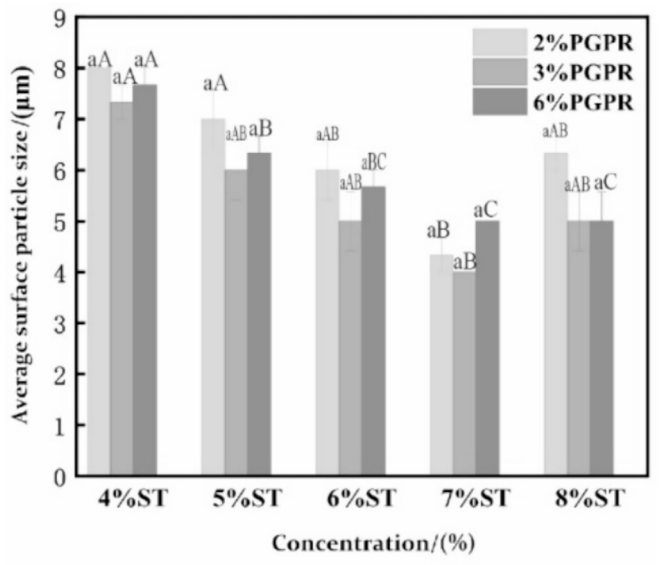

Fig. 4. Average surface particle sizes of gel emulsions prepared with 2%, 3% and 6% PGPR and different ST concentrations (Aqueous solution concentrations of all samples constant to be 65%). Samples designated with different lowercase letters indicate a significant difference ($P<0.05$) when compared between different concentrations of PGPR. Samples designated with different capital letters indicate a significant difference ($P<0.05$) when compared between different concentrations of ST.

increased noticeably as the PGPR concentration increased. At a PGPR concentration of 2%, rod-shaped ST crystals were dispersed within the continuous phase. With a 3% PGPR concentration, dispersed rod-shaped crystals within the continuous phase and white circular crystalline rings surrounding the droplets were observed. At 6% PGPR in gel emulsions with modest ST concentrations (4–6%), white circular crystalline rings were predominantly observed around the droplets. When the ST concentration exceeded 6%, the system displayed dispersed rod-shaped crystals in a continuous phase, with white circular crystalline rings surrounding the droplets. This observation is consistent with the findings of the optical microstructure analysis. At higher PGPR concentrations, the crystal structure of the emulsion systems prepared with low ST concentrations mainly consisted of crystalline rings and failed to form a gel-like emulsion. However, at higher ST concentrations, the system displayed both rod-shaped crystals and white crystalline rings, resulting in enhanced stability and a gel-like consistency.

Based on our previous FTIR analysis (Tang et al., 2022), Stigmasterol forms intermolecular hydrogen bonds in rapeseed oil-based gel emulsions. The stigmasterol crystals are attracted to each other through hydrogen bonding, leading to the formation of a crystalline three-dimensional network. This network formation proceeds through the pathway of aggregation-nucleation-growth, resulting in the spontaneous formation of supramolecular aggregates that contribute to the gel emulsion structure. As an amphiphilic emulsifier, PGPR can establish hydrogen bonds with water through its hydrophilic portion, whereas its hydrophobic portion can anchor onto the curved chains of fatty acids in vegetable oils (Ghosh & Rousseau, 2011). This dual affinity allows PGPR to adsorb at the oil-water interface, stabilizing the emulsion droplets. When emulsions are prepared with a specific concentration of PGPR, intense interactions between the water and oil phases in the emulsion system lead to the formation of interfacial crystals that stabilize the emulsion droplets (also known as Pickering interface stabilization). So the number of crystals continue to increase with increasing PGPR concentration. Consequently, the white crystalline circles observed in our gel emulsion system were interfacial crystals formed by PGPR within the emulsion. The distinct crystallization modes of ST and PGPR significantly affected the formation mechanism and properties of the gel emulsion, as suggested by these results. Gel emulsions primarily demonstrate two stabilization mechanisms: Pickering interface stabilization and crystalline network stabilization (Yang et al., 2017). Notably, gel emulsions consisting of 2% PGPR and ST were primarily stabilized by a continuous phase network structure. The gel emulsion comprising 3% PGPR and ST was primarily stabilized by both Pickering interface stabilization and a continuous-phase crystal network structure. Conversely, the gel emulsion containing 6% PGPR and ST was primarily stabilized via Pickering interface stabilization. Previous research suggests gel emulsions stabilized by a combination of Pickering and network mechanisms exhibit superior physical and chemical properties (Ghosh, Tran, & Rousseau, 2011; Ghosh & Rousseau, 2012; Wan, Xia, Guo, & Zeng, 2021).

3.4. Surface mean particle size analysis

The variation in the gel emulsion surface mean particle size ($d_{3,2}$) (Fig. 4) revealed that the gel emulsion droplet size decreased within the range of 4–7% as the ST concentration increased. However, at a concentration of 8%, the particle size of emulsion gel droplets increased significantly. This may have been the result of excessively high ST concentrations. Upon mixing ST with rapeseed oil and subsequent heating for dissolution, a portion of ST swiftly formed crystals in the oil, leading to an insufficient presence of ST crystals at the interface to effectively stabilize the droplets during high shear. This phenomenon affected the dispersion effect, resulting in a relatively large $d_{3,2}$ in the gel emulsion. Initially, as the concentration of PGPR increased, the $d_{3,2}$ of the emulsion gel droplets decreased and then increased. Specifically, at a PGPR concentration of 2%, the droplet distribution in the gel emulsion was asymmetrical, with $d_{3,2}$ ranging from 4.3 to 8 μm. The droplet $d_{3,2}$ values varied from 4 to 7.3 μm in the gel emulsion at a PGPR concentration of 3%, while the particle size $d_{3,2}$ values in the 6% PGPR gel emulsion ranged from 5 to 7.8 μm. In emulsions with low ST concentrations (4–6%), the average particle size was large. However, when the

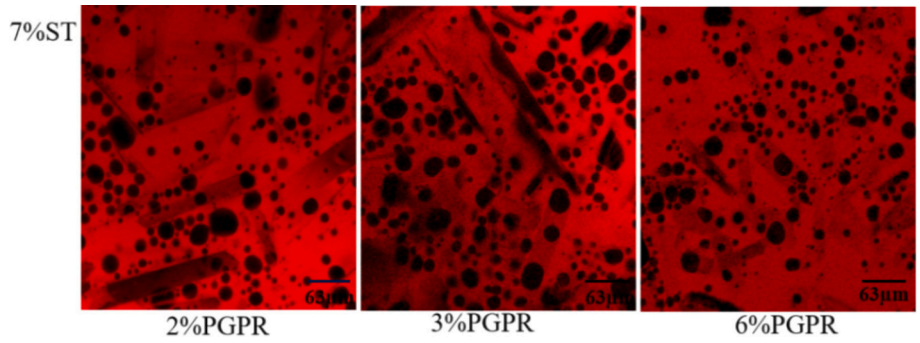

Fig. 5. Confocal laser microscopy images of gel emulsions prepared with 2%, 3%, and 6% PGPR and 7% ST (Aqueous solution concentrations of all samples constant to be 65%). Scale bar = 63 μm.

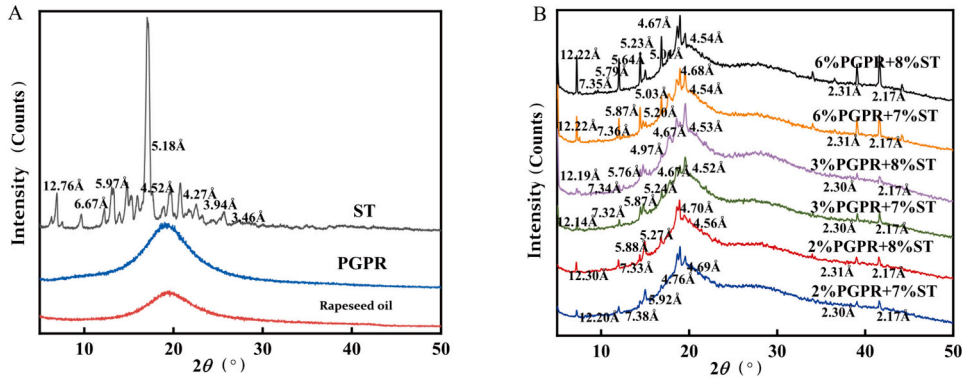

Fig. 6. (A) X-ray diffraction (XRD) patterns of rapeseed oil, ST, and PGPR; (B) XRD patterns of gel emulsions prepared with 2%, 3% and 6% PGPR in combination with ST.

ST concentration exceeded 6%, the average droplet size decreased, indicating increased stability in the system. This suggests that the primary stabilization mechanism in emulsions prepared with low ST and high PGPR concentrations was Pickering interface stabilization, which meant that they were structurally unstable and incapable of forming a gel emulsion, thereby resulting in an increase in particle size. Conversely, when the ST concentration exceeded 6%, the main stability mechanism in the emulsion system shifted to Pickering interface stabilization and the formation of a continuous-phase crystal network structure, resulting in a more stable system and smaller average droplet size. Gel emulsions prepared with 3% PGPR had relatively smaller $d_{3,2}$ values than those prepared with 2% or 6% PGPR. This may be because of the gel emulsion formation mechanism, in which the gel emulsion prepared with 3% PGPR stabilized the droplets by forming a crystalline shell at the droplet interface. This formed a crystal network in the continuous phase to restrict droplet-to-droplet contact, thereby preventing droplet aggregation and resulting in a relatively smaller droplet size, indicating a stronger structural appearance.

3.5. Laser confocal scanning microstructure analysis

Fig. 5 illustrates laser confocal scanning microscopy images of gel emulsions prepared with PGPR concentrations of 2%, 3%, and 6% at a 7% concentration of ST. The oil phase of the gel emulsion displayed red fluorescence under 488 nm excitation light, and black droplets were disseminated throughout the oil phase. This indicates that the PGPR and ST-formed gel emulsions were water-in-oil (W/O) emulsions. In addition, the droplet distribution in the gel emulsion prepared with 3% PGPR was more uniform than the distributions in those prepared with 2% and 6% PGPR. This result is consistent with the optical microscopy and polarized light microscopy observations.

3.6. XRD analysis

The crystal structure of the gel emulsion system was analyzed using XRD. To analyze the effects of PGPR and ST concentrations on the crystal phase of the gel emulsions, gel emulsions were prepared using 2%, 3%,

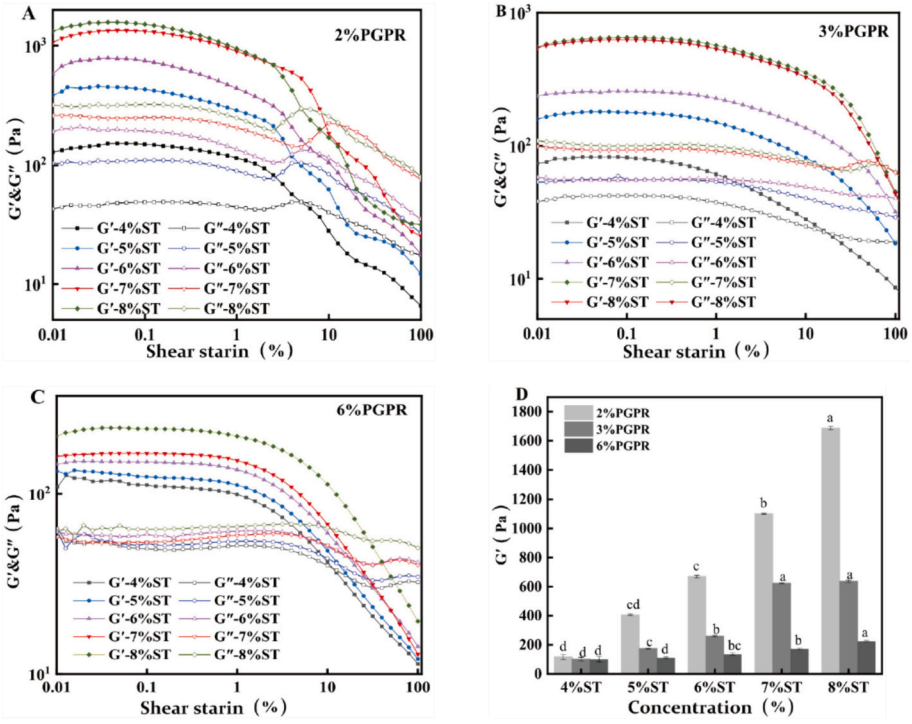

Fig. 7. (A–C) Strain scanning curves of gel emulsions prepared with 2%, 3%, and 6% PGPR and different ST concentrations; (D) G′ values of gel emulsions prepared with 2%, 3%, and 6% PGPR and different ST concentrations. Different letters indicate significant differences between groups ($P<0.05$).

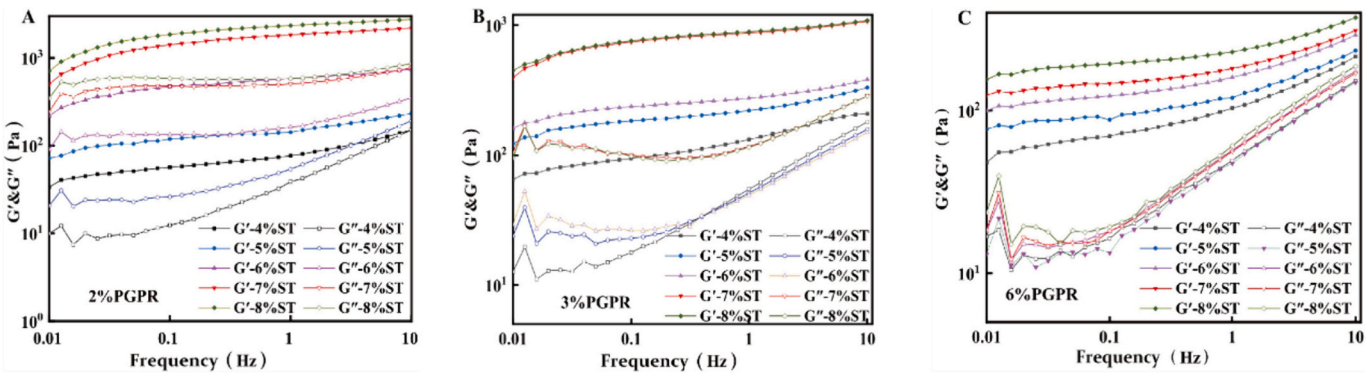

Fig. 8. (A–C) Frequency scanning curves of gel emulsions prepared with 2%, 3%, and 6% PGPR and different ST concentrations.

and 6% PGPR, along with 7% and 8% ST in rapeseed oil. As shown in Fig. 6A and B, rapeseed oil, PGPR, and different gel emulsions exhibited a broad peak at 4.5 Å, which is related to the main amorphous structure. According to the XRD partterns of different gel emulsions, a sharp peak at approximately 4.6 Å was observed, indicating the presence of β-crystals. Similar crystal peaks were observed in the gel emulsion as those observed in ST gel in previous research (Tang et al., 2022), with broad peaks appearing at 4.26 Å and 4.52 Å. This indicated the presence of α- and β-crystals in the gel emulsion system. Notably, the crystalline peaks in the emulsion shifted toward shorter pitches. Specifically, the ST crystalline peak at 12.76 Å shifted to 12.32 Å in the emulsion, and new short-spacing peaks emerged at 2.31 Å and 2.20 Å. Previous studies have associated long-spacing peaks with molecular lamination and short-spacing peaks with molecular lateral stacking (Gong et al., 2019). With increasing ST and PGPR concentrations, the short-spacing peaks in the gel emulsion increased, and the positions of some peaks shifted, indicating a rearrangement of molecular stacking within the system. This resulted in a denser arrangement of rod-shaped ST crystals on the droplet surface and interface crystals formed by PGPR.

3.7. Rheological analysis

3.7.1. Strain sweep analysis

Further rheological experiments were conducted to investigate the effects of ST and PGPR concentrations on the macroscopic properties of gel emulsions. Fig. 7 A–C depicts the results of the strain sweep of the gel emulsions prepared with 2%, 3%, and 6% PGPR at various ST concentrations. With the increase in strain amplitude, G' and G" initially exhibit a clear plateau, indicating the state of linear viscoelasticity(Xia et al., 2022). All gel emulsion samples exhibited $G' > G''$ within the linear viscoelastic range (0.01–0.1%). Nonetheless, as the strain increased, the value of G′ decreased, and a crossover point occurred between G′ and G″, indicating the disintegration of the gel emulsion network structure(Sun et al., 2022). The gel emulsion made with 2% PGPR and ST had the lowest crossover value (The strain value at G"/G' cross-over point in the strain sweep) between G′ and G″, whereas the gel emulsion made with 3% PGPR and ST had the highest crossover value. This could be attributed to the fact that the gel emulsion prepared with 2% PGPR and ST stabilized the emulsion droplets primarily through crystal networks, resulting in a system with weak overall stability. Han, et al. found that the higher the crossover value, the stronger the gel structure(Han, Ren, Shen, Yang, & Li, 2024). As the shear stress increased, the droplets tended to aggregate, and the mechanical strength of the system network decreased, resulting in the destruction of the network structure.

Fig. 7D illustrates the variation of gel emulsion G′ values with respect to PGPR and ST concentrations. The G′ value of the gel emulsion increased as the ST concentration increased and decreased as the PGPR concentration increased. The gel emulsion prepared with 2% PGPR exhibited the highest G′ value, whereas the gel emulsion prepared with 6% PGPR exhibited the lowest G′ value, indicating that the gel network structure formed by ST in the continuous phase was predominantly responsible for the mechanical strength of the gel emulsion. This further demonstrated that the formation mechanism of the gel emulsion influenced its mechanical properties. Gel emulsions stabilized by a continuous-phase crystal network structure mechanism (2% PGPR) had high mechanical strength but were susceptible to structural damage because of their unstable emulsion systems. Gel emulsions stabilized by both Pickering interface stabilization and continuous-phase crystal network structure stabilization (3% PGPR) exhibited enhanced mechanical strength and more stable internal structures, with reduced susceptibility to damage.

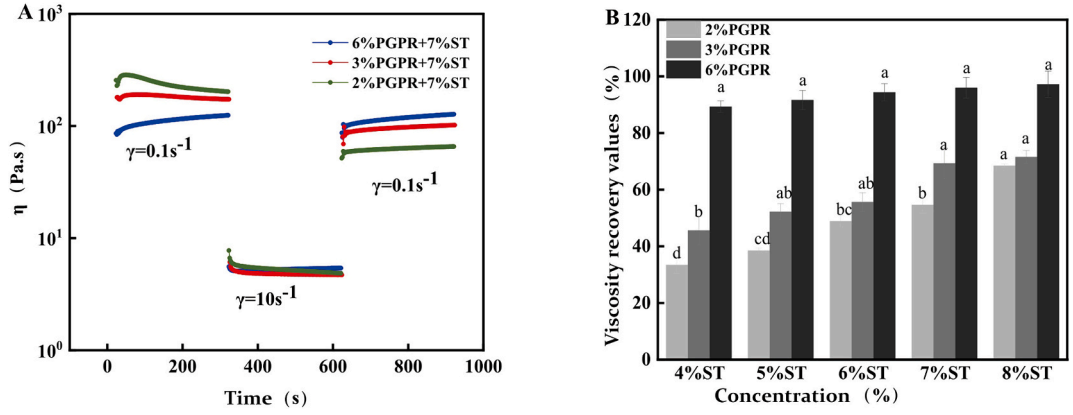

Fig. 9. (A) Thixotropic recovery curves represented by gel emulsions prepared with 2%, 3%, and 6% PGPR and 7% ST; (B) Viscosity recovery values of gel emulsions prepared with 2%, 3%, and 6% PGPR and different ST concentrations. Different letters indicate significant differences between groups ($P<0.05$).

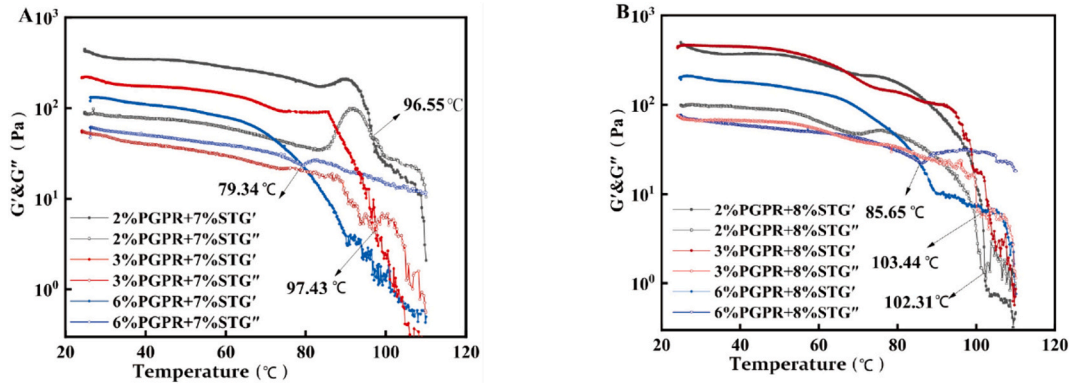

Fig. 10. (A) Temperature scanning curves of gel emulsions prepared with 2%, 3%, and 6% PGPR with 7% ST; (B) Temperature scanning curves of gel emulsions prepared with 2%, 3%, and 6% PGPR with 8% ST.

3.7.2. Frequency sweep analysis

Frequency sweeps of the gel emulsions prepared with 2%, 3%, and 6% PGPR at various ST concentrations are depicted in Fig. 8 A–C. During the frequency scan, the G′ values of all gel emulsions were greater than those of G″, indicating a predominantly elastic behavior. The G′ value of the gel emulsion increased as the ST concentration increased and decreased as the PGPR concentration increased. Furthermore, the modulus of all gel emulsions rose as the scanning frequency increased, suggesting that all gel emulsions exhibited solid-like properties(Chu et al., 2024). Consistent with the results of the strain sweep, the gel emulsion prepared with 2% PGPR and ST exhibited the highest G′ value, whereas the gel emulsion prepared with 6% PGPR and ST exhibited the lowest G′ value. Additionally, the G′ and G″ values of gel emulsions prepared with 2% and 3% PGPR increased marginally with increasing frequency, whereas the G′ and G″ values of gel emulsions prepared with 6% PGPR changed significantly with increasing frequency. This was because of the high concentrations of PGPR and ST in the gel emulsion, which permitted the formation of a greater number of interface crystals. As the scanning frequency increased, the interface crystals formed a cross-linked network within the gel emulsion system, imparting a relatively elastic network structure and causing significant variations in the G′ and G″ values of the samples.

3.7.3. Thixotropic recovery scan analysis

Using a three-interval time test, the effect of PGPR and ST concentrations on the structural recovery efficacy of the gel emulsion were investigated. Fig. 9A depicts the variation in the viscosity of gel emulsions prepared with 2%, 3%, and 6% PGPR and 7% ST at various shear rates. After undergoing shearing at three distinct shear rates, the viscosity of the gel emulsion gradually recovered. Ideally, materials exhibit a desired thixotropic recovery when the peak viscosity in the third interval recovers at least 70% of its initial measurement taken after the first interval (Menard & Menard, 2006). Fig. 9B shows the viscosity recovery values of the gel emulsions prepared with 2%, 3%, and 6% PGPR and various ST concentrations following the three shearing stages. The results revealed a positive correlation between the viscosity recovery values of the gel emulsion and the ST and PGPR concentrations. The viscosity recovery values of the gel emulsions increased with increasing ST concentration when the PGPR concentration was 2% or 3%. When the ST concentration was 8%, the gel emulsion viscosity recovery values were 68.49% and 71.53%. Conversely, at a PGPR concentration of 6%, the gel emulsion exhibited significantly higher viscosity recovery, reaching 97.21%, with the ST concentration showing minimal impact. This phenomenon is attributed to the higher PGPR concentration, which elevates the interfacial tension within the gel emulsion, facilitating the formation of a dense interface between the oil and water phases. Consequently, the gel emulsion can rapidly restore its viscosity, even after undergoing multiple stages of shearing.

The combination of polarized light microscopy and frequency sweep analysis indicates that gel emulsions prepared with 2% PGPR and varying ST concentrations primarily rely on the crystalline network structure of ST within the continuous phase to uphold overall system stability. While possessing substantial mechanical strength, these emulsions exhibit weaker viscoelastic recovery. Conversely, gel emulsions formulated with 6% PGPR and varied ST concentrations predominantly depend on Pickering interface stabilization, resulting in lower mechanical strength but higher viscoelasticity. Despite undergoing multiple shearing phases, these emulsions can recover their viscoelastic properties efficiently. The gel emulsions prepared with 3% PGPR and varying concentrations of ST relied on both Pickering interface stabilization and continuous-phase crystal network stabilization, resulting in a denser network structure that was difficult to disrupt. These emulsions exhibited excellent mechanical strength and thixotropic recovery characteristics.

3.7.4. Temperature scan analysis

The effects of the PGPR and ST concentrations on the temperature stability of the gel emulsion were analyzed using a temperature scan. Fig. 10A and B displays the results of the temperature scan for gel emulsions prepared with 2%, 3%, and 6% PGPR and 7% or 8% ST. As the scanning temperature increased, both the G′ and G″ of the gel emulsion progressively decreased. Upon reaching 60 °C, G' and G" exhibited a rapid decline, marking the onset of a critical phase transition temperature, denoted as the crossover point between G' and G". Within the temperature scan range, there was a correlation between the concentrations of PGPR and ST and the critical phase transition temperature of the gel emulsion. The critical phase transition temperatures for gel emulsions prepared with 2% PGPR and 7% or 8% ST were 96.55 °C and 102.31 °C, respectively. The critical phase transition temperatures for gel emulsions prepared with 3% PGPR and 7% or 8% ST were 97.43 °C and 103.44 °C, respectively. The critical phase transition temperatures for gel emulsions prepared with 6% PGPR and 7% or 8% ST were 79.34 °C and 85.65 °C, respectively. These results further demonstrate that gel emulsions stabilized by both Pickering interface stabilization and a continuous-phase crystal network (3% PGPR) had enhanced thermal stability. Moreover, these findings align with a previous investigation (Wijarnprecha, De Vries, Santiwattana, Sonwai, & Rousseau, 2019), which suggested that a combination of core-shell and network structures imparts additional rigidity and enhanced stability.

3.8. Differential scanning calorimetry (DSC) thermodynamic analysis

Thermal analysis using DSC was performed to determine the effects of PGPR and ST concentrations on the thermal stability of the gel emulsions. Thermal stability reflects the stability of a gel emulsion system and its resistance to decomposition at high temperatures, a

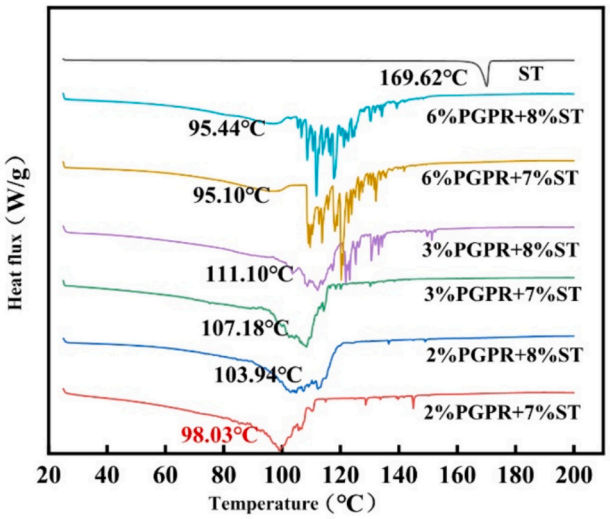

Fig. 11. Differential scanning calorimetry (DSC) heat maps of gel emulsions containing 2%, 3%, and 6% PGPR with 7% and 8% ST.

crucial property of fat-based products (De Oliveira, Ribeiro, & Kieckbusch, 2015; Paximada, Howarth, & Dubey, 2021). During the temperature change, the gel emulsion underwent phase transitions and crystallization, as indicated by the endothermic peaks observed at high temperatures. Fig. 11 illustrates that pure ST exhibited a comparatively high melting point of 169.62 °C. Additionally, the melting point of gel emulsions formulated with ST increased proportionally with its concentration. This phenomenon can be attributed to the inherently high melting point of ST, leading to gel emulsions with elevated phase transition temperatures and enhanced thermal stability. Moreover, the gel emulsions comprising 3% PGPR and 7% or 8% ST exhibited relatively high peak melting temperatures of 107.18 °C and 111.10 °C, respectively. The minimal melting temperatures of the gel emulsions prepared with 6% PGPR and 7% or 8% ST were 95.10 °C and 95.44 °C, respectively. These results are consistent with the findings of the temperature scan analysis.

3.9. Stability analysis

3.9.1. Physical stability analysis

For prospective applications in the food, pharmaceutical, and cosmetic industries, it is crucial to investigate the effects of PGPR and ST concentrations on the physical stability of gel emulsions. Fig. 12A–C depict gel emulsions prepared with 2%, 3%, and 6% PGPR and varying ST concentrations after 30 d of storage at room temperature and 24 h of oven storage at 50 °C, 60 °C, and 70 °C, respectively. After 30 d at room temperature or 24 h in the oven at 50 °C and 60 °C, gel emulsions formulated with 2% PGPR and various ST concentrations maintained their gel-like consistency and adhered to the bottom of the vial (Fig. 12A). However, at ST concentrations of 4% and 5%, the gel emulsions lost their gel-like structure after 24 h of oven storage at 70 °C. Fig. 12B demonstrated that gel emulsions prepared with 3% PGPR and various concentrations of ST retained their gel-like state and adhered to the bottom of the vial after 30 d of storage at room temperature or 24 h of oven storage at 50 °C, 60 °C, and 70 °C. This indicated that the gel emulsions exhibited excellent thermal stability, which was consistent with the results of the temperature scan and DSC analysis. However, as shown in Fig. 12C, gel emulsions prepared with 6% PGPR and various ST concentrations exhibited instability. Only the gel emulsions prepared with high concentrations (7% and 8%) of ST retained their gel-like structure after 30 d of storage at room temperature or 24 h of oven storage at 50 °C. However, at 70 °C, the gel structure of the emulsions within the chosen ST concentration range was disrupted, and the system failed to maintain its gel-like state.

As depicted in Fig. 13A–C, the particle size distributions ($d_{3,2}$) of the gel emulsions prepared with 2%, 3%, and 6% PGPR and varying concentrations of ST were observed and measured using an optical microscope. Following 30 d of storage at room temperature or 24 h of oven storage at 50 °C, 60 °C, and 70 °C, the $d_{3,2}$ values of the gel emulsions decreased with an increase in ST concentration. Gel emulsions prepared with 2% and 6% PGPR exhibited notable differences in $d_{3,2}$, compared with that in freshly prepared gel emulsions, whereas those prepared with 3% PGPR exhibited relatively minor changes in $d_{3,2}$ under various

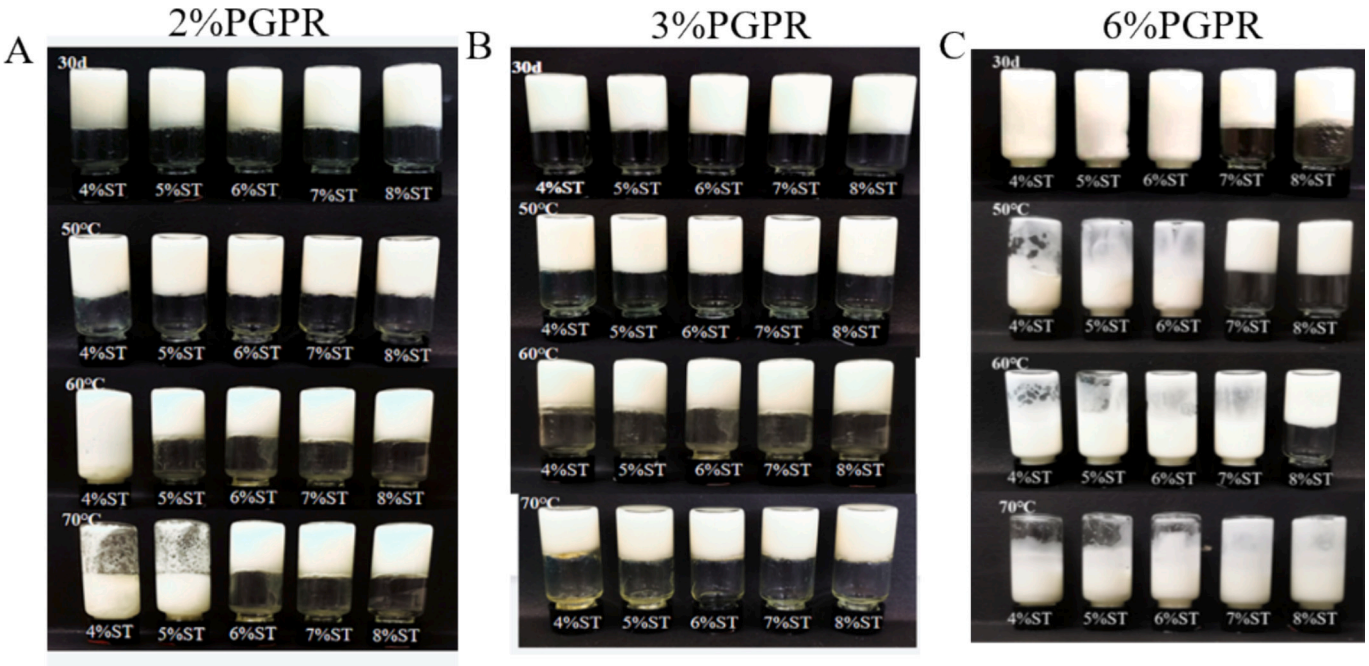

Fig. 12. Appearance of gel emulsions prepared with 2% (A), 3% (B), and 6% (C) PGPR and different ST concentrations after storage at room temperature for 30 d and in an oven at 50 °C, 60 °C, and 70 °C for 24 h.

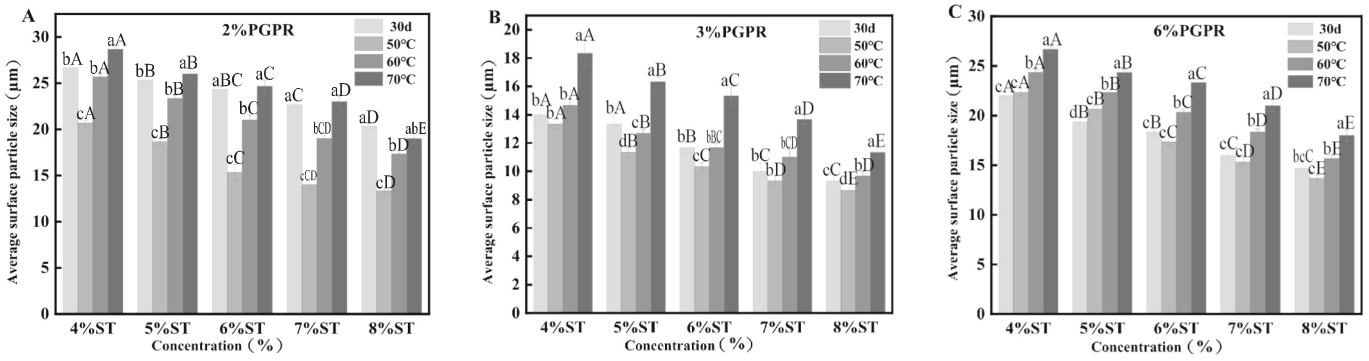

Fig. 13. Average surface particle sizes of gel emulsions prepared with 2% (A), 3% (B), and 6% (C) PGPR and different ST concentrations after storage at room temperature for 30 d and in ovens at 50 °C, 60 °C, and 70 °C for 24 h. Samples designated with different lower-case letters indicate a significant difference ($P<0.05$) when compared between different heating methods. Samples designated with different capital letters indicate a significant difference ($P<0.05$) when compared between different concentrations of ST.

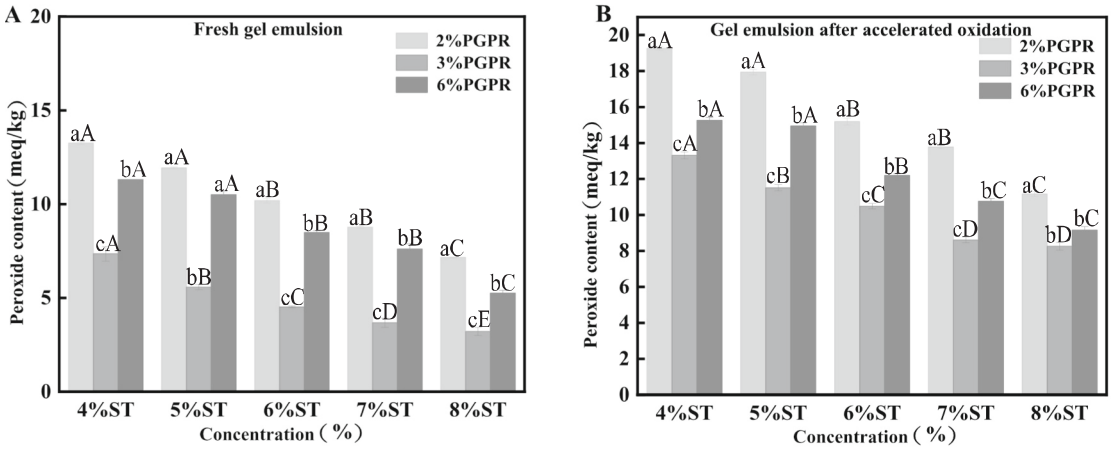

Fig. 14. (A) Changes in peroxide content in fresh gel emulsions prepared with 2%, 3%, and 6% PGPR and different ST concentrations; (B) Changes in peroxide content after accelerated oxidation of gel emulsions prepared with 2%, 3%, and 6% PGPR and different ST concentrations. Samples designated with different lower-case letters indicate a significant difference ($P<0.05$) when compared between different concentrations of PGPR. Samples designated with different capital letters indicate a significant difference ($P<0.05$) when compared between different concentrations of ST.

storage conditions.

Gel network systems stabilized by the combined action of the Pickering interface and the crystalline network (3% PGPR) were more stable than gel network systems stabilized solely by the crystalline network (2% PGPR) or the Pickering interface (6% PGPR). Another study (Lee, Tan, Ravanfar, & Abbaspourrad, 2019) arrived at similar conclusions regarding gel emulsions prepared with beeswax and glyceryl monocaprylate (GMO). The combined effect of Pickering interface stabilization and crystalline network formation contributed to a more stable emulsion system by impeding droplet sedimentation, coalescence, and flocculation.

3.9.2. Oxidative stability analysis

Emulsion products may experience rapid expiration because of lipid oxidation (Bao & Pignitter, 2023). To determine the effect of the PGPR and ST concentrations on the oxidative stability of the emulsion, the peroxide contents of the fresh gel emulsion and oven-accelerated oxidized gel emulsion were determined. Fig. 14A shows the amount of peroxide in the fresh gel emulsion. The peroxide content of the gel emulsion decreased with increasing ST concentration, whereas it initially decreased and then increased with increasing PGPR concentration. Gel emulsions formulated with 2% PGPR and 6% PGPR with ST contained more peroxide than those formulated with 3% PGPR and ST. This suggests that gel emulsions prepared with 3% PGPR and ST formed a structural network and crystallized the interface in the lipid phase, which had a greater effect on delaying lipid oxidation.

As depicted in Fig. 14B, the peroxide content of the gel emulsions was determined after 5 d of storage in an oven at 60 °C. After accelerated oven oxidation, the peroxide content of the gel emulsions increased compared with that of the freshly prepared gel emulsion. However, as the ST concentration increased, the peroxide content decreased. This is because ST is an effective antioxidant (Hussein et al., 2022) and can exert its antioxidant effect during the accelerated oxidation process, reducing peroxide production and delaying partial oxidation of the lipid phase. In addition, the gel emulsion prepared with 3% PGPR + ST contained significantly less peroxide than those prepared with 2% and 6% PGPR + ST. This indicated that the gel emulsion prepared with 3% PGPR and varying concentrations of ST had a densely distributed network structure, excellent thermal stability, and could withstand the high-temperature accelerated oxidation process without structural degradation, thereby delaying lipid oxidation by restricting oil flow and migration (Lim, Hwang, & Lee, 2017).

4. Conclusions

In this study, we investigated the impact of varying concentrations of ST and PGPR on the structure and properties of gel emulsions. The results showed that incorporating 6% ST alone effectively stabilized the water phase of the 45 wt% emulsion. When 2% PGPR was introduced, a stable W/O gel emulsion formed with 4% ST, maintaining a 65 wt%

water phase ratio. Further analysis of ST and PGPR concentrations at this ratio revealed that increasing ST concentration led to a denser network structure and improved stability of the gel emulsion. At a 65 wt % water phase ratio, the gel emulsion containing 2% PGPR and ST achieved stabilization through a continuous phase network structure. The gel emulsion prepared with 3% PGPR and ST was strengthened and stabilized via the Pickering interface stabilization and continuous-phase crystal network stabilization mechanisms. The 6% PGPR and ST gel emulsions were predominantly stabilized via the Pickering interface stabilization mechanism. Compared with the gel emulsions formed with 2% and 6% PGPR and ST, the 3% emulsifier and ST gel emulsion exhibited superior rheological strength and viscosity recovery. The gel emulsion displayed a maximal melting temperature of 111.1 °C, indicating excellent thermal stability. It maintained its gel-like consistency during high-temperature storage, with minimal changes in particle size and a pronounced delay in lipid oxidation.

Additionally, W/O gel emulsions formulated with ST and PGPR as co-emulsifiers exhibited low trans-fat and saturated fatty acid content. Incorporating water into the gel system reduced its calorie content by leveraging its 65% fat composition. This study paves the way for developing novel W/O emulsions with enhanced stability, potentially replacing puff pastry fat and margarine in culinary applications.

Declaration of competing interest

The authors declare no conflicts of interest.

Data availability

Data will be made available on request.

Acknowledgments

This work was supported by the National Natural Science Foundation of China [No. 31671858] and Natural Science Foundation of Hunan Province [2022JJ30295]. In addition, the APC was funded by Hunan Agricultural University.

References

Bai, L., Huan, S., Rojas, O. J., & McClements, D. J. (2021). Recent innovations in emulsion science and technology for food applications. *Journal of Agricultural and Food Chemistry, 69*, 8944–8963. https://doi.org/10.1021/acs.jafc.1c01877

Bao, Y., & Pignitter, M. (2023). Mechanisms of lipid oxidation in water-in-oil emulsions and oxidomics-guided discovery of targeted protective approaches. *Comprehensive Reviews in Food Science and Food Safety, 22*, 2678–2705. https://doi.org/10.1111/1541-4337.13158

Bascuas, S., Morell, P., Hernando, I., & Quiles, A. (2021). Recent trends in oil structuring using hydrocolloids. *Food Hydrocolloids, 118*, Article 106612. https://doi.org/10.1016/j.foodhyd.2021.106612

Brühl, L. (1997). Official methods and recommended practices of the American oil chemist's society, physical and chemical characteristics of oils, fats and waxes. In Section I (Ed.), *The AOCS Methods Editor and the AOCS Technical Department* (p. 54). Champaign: AOCS Press. https://doi.org/10.1002/lipi.19970990510, 1996. Lipid / Fett. Champaign: AOCS Press, 99, 197–197.

Cercaci, L., Rodriguez-Estrada, M. T., Lercker, G., & Decker, E. A. (2007). Phytosterol oxidation in oil-in-water emulsions and bulk oil. *Food Chemistry, 102*, 161–167. https://doi.org/10.1016/j.foodchem.2006.05.010

Chen, Z., Bian, F., Cao, X., Shi, Z., & Meng, Z. (2023). Novel bigels constructed from oleogels and hydrogels with contrary thermal characteristics: Phase inversion and 3D printing applications. *Food Hydrocolloids, 134*, Article 108063. https://doi.org/10.1016/j.foodhyd.2022.108063

Chew, S. C. (2020). Cold-pressed rapeseed (Brassica napus) oil: Chemistry and functionality. *Food Research International, 131*, Article 108997. https://doi.org/10.1016/j.foodres.2020.108997

Choi, S. J., Decker, E. A., & McClements, D. J. (2009). Impact of iron encapsulation within the interior aqueous phase of water-in-oil-in-water emulsions on lipid oxidation. *Food Chemistry, 116*, 271–276. https://doi.org/10.1016/j.foodchem.2009.02.045

Chu, Z., Li, X., Han, R., Yang, Q., Fei, P., Zhang, H., … Liu, J. (2024). Effect of ultrasound on heated soybean isolate protein-soybean oligosaccharide glycation conjugate acid-induced emulsion gels and their applications as carriers of zeaxanthin. *Food Hydrocolloids, 150*, 109719. https://doi.org/10.1016/j.foodhyd.2023.109719

Cui, L., Guo, J., & Meng, Z. (2023). A review on food-grade-polymer-based O/W emulsion gels: Stabilization mechanism and 3D printing application. *Food Hydrocolloids, 139*, Article 108588. https://doi.org/10.1016/j.foodhyd.2023.108588

De Oliveira, G. M., Ribeiro, A. P. B., & Kieckbusch, T. G. (2015). Hard fats improve technological properties of palm oil for applications in fat-based products. *LWT – Food Science and Technology, 63*, 1155–1162. https://doi.org/10.1016/j.lwt.2015.04.040

Dickinson, E. (2012). Emulsion gels: The structuring of soft solids with protein-stabilized oil droplets. *Food Hydrocolloids, 28*, 224–241. https://doi.org/10.1016/j.foodhyd.2011.12.017

Gao, Z., Maloney, D. J., Dedkova, L. M., & Hecht, S. M. (2008). Inhibitors of DNA polymerase β: Activity and mechanism. *Bioorganic and Medicinal Chemistry, 16*, 4331–4340. https://doi.org/10.1016/j.bmc.2008.02.071

Ge, S., Xiong, L., Li, M., Liu, J., Yang, J., Chang, R., Liang, C., & Sun, Q. (2017). Characterizations of Pickering emulsions stabilized by starch nanoparticles: Influence of starch variety and particle size. *Food Chemistry, 234*, 339–347. https://doi.org/10.1016/j.foodchem.2017.04.150

Ghosh, S., & Rousseau, D. (2011). Fat crystals and water-in-oil emulsion stability. *Current Opinion in Colloid and Interface Science, 16*, 421–431. https://doi.org/10.1016/j.cocis.2011.06.006

Ghosh, S., & Rousseau, D. (2012). Triacylglycerol interfacial crystallization and shear structuring in water-in-oil emulsions. *Crystal Growth & Design, 12*(10), 4944–4954. https://doi.org/10.1021/cg300872m

Ghosh, S., Tran, T., & Rousseau, D. (2011). Comparison of Pickering and network stabilization in water-in-oil emulsions. *Langmuir, 27*(11), 6589–6597. https://doi.org/10.1021/la200065y

Gong, N., Wang, Y., Zhang, B., Yang, D., Du, G., & Lu, Y. (2019). Screening, preparation and characterization of diosgenin versatile solvates. *Steroids, 143*, 18–24. https://doi.org/10.1016/j.steroids.2018.11.016

Han, C., Yang, X., & Li, L. (2024). Improvement of physicochemical properties and quercetin delivery ability of fermentation-induced soy protein isolate emulsion gel processed by ultrasound. *Ultrasonics Sonochemistry, 106902*. https://doi.org/10.1016/j.ultsonch.2024.106902

Hussein, H.-A. A., Alshammari, S. O., Elkady, F. M., Ramadan, A. A., Kenawy, S. K. M., & Abdelkawy, A. M. (2022). Radio-protective effects of stigmasterol on wheat (Triticum aestivum L.) plants. *Antioxidants, 11*, 1144. https://doi.org/10.3390/antiox11061144

Kaur, N., Chaudhary, J., Jain, A., & Kishore, L. (2011). Stigmasterol: A comprehensive review. *International Journal of Pharmaceutical Sciences and Research, 2*, 2259.

Lee, M. C., Tan, C., Ravanfar, R., & Abbaspourrad, A. (2019). Ultrastable water-in-oil high internal phase emulsions featuring interfacial and biphasic network stabilization. *ACS Applied Materials and Interfaces, 11*, 26433–26441. https://doi.org/10.1021/acsami.9b05089

Lim, J., Hwang, H. S., & Lee, S. (2017). Oil-structuring characterization of natural waxes in canola oil oleogels: Rheological, thermal, and oxidative properties. *Applied Biological Chemistry, 60*, 17–22. https://doi.org/10.1007/s13765-016-0243-y

Lin, D., Kelly, A. L., & Miao, S. (2020). Preparation, structure-property relationships and applications of different emulsion gels: Bulk emulsion gels, emulsion gel particles, and fluid emulsion gels. *Trends in Food Science and Technology, 102*, 123–137. https://doi.org/10.1016/j.tifs.2020.05.024

Lin, Q., Liang, R., Zhong, F., Ye, A., & Singh, H. (2021). In vivo oral breakdown properties of whey protein gels containing OSA-modified-starch-stabilized emulsions: Impact of gel structure. *Food Hydrocolloids, 113*, Article 106361. https://doi.org/10.1016/j.foodhyd.2020.106361

Liu, C., Li, Y., Liang, R., Sun, H., Wu, L., Yang, C., & Liu, Y. (2023). Development and characterization of ultrastable emulsion gels based on synergistic interactions of xanthan and sodium stearoyl lactylate. *Food Chemistry, 400*, Article 133957. https://doi.org/10.1016/j.foodchem.2022.133957

Liu, Y., Ma, S., Xia, H., Guo, S., & Zeng, C. (2022). Edible oleogels stabilized solely by stigmasterol: Effect of oil type and gelator concentration. *Journal of the Science of Food and Agriculture, 102*, 4759–4769. https://doi.org/10.1002/jsfa.11841

Mao, L., Calligaris, S., Barba, L., & Miao, S. (2014). Monoglyceride self-assembled structure in O/W emulsion: Formation, characterization and its effect on emulsion properties. *Food Research International, 58*, 81–88. https://doi.org/10.1016/j.foodres.2014.01.042

Márquez, A. L., Medrano, A., Panizzolo, L. A., & Wagner, J. R. (2010). Effect of calcium salts and surfactant concentration on the stability of water-in-oil (w/o) emulsions prepared with polyglycerol polyricinoleate. *Journal of colloid and interface science, 341*(1), 101–108. https://doi.org/10.1016/j.jcis.2009.09.020

Menard, K. P., Menard, N., & Dynamic mechanical analysis. (2006). *Encyclopedia of analytical Chemistry: Applications. Theory and Instrumentation* (pp. 1–25).

Navarro, A., De Las Heras, B., & Villar, A. (2001). Anti-inflammatory and immunomodulating properties of a sterol fraction from Sideritis foetens Clem. *Biological and Pharmaceutical Bulletin, 24*, 470–473. https://doi.org/10.1248/bpb.24.470

Okuro, P. K., Gomes, A., Costa, A. L. R., Adame, M. A., & Cunha, R. L. (2019). Formation and stability of W/O-high internal phase emulsions (HIPEs) and derived O/W emulsions stabilized by PGPR and lecithin. *Food Research International, 122*, 252–262. https://doi.org/10.1016/j.foodres.2019.04.028

Paximada, P., Howarth, M., & Dubey, B. N. (2021). Double emulsions fortified with plant and milk proteins as fat replacers in cheese. *Journal of Food Engineering, 288*, Article 110229. https://doi.org/10.1016/j.jfoodeng.2020.110229

Poyato, C., Astiasarán, I., Barriuso, B., & Ansorena, D. (2015). A new polyunsaturated gelled emulsion as replacer of pork back-fat in burger patties: Effect on lipid

composition, oxidative stability and sensory acceptability. *LWT – Food Science and Technology, 62*, 1069–1075. https://doi.org/10.1016/j.lwt.2015.02.004

Price, R., Gray, D., Watson, N., Vieira, J., & Wolf, B. (2022). Linking the yield stress functionality of polyglycerol polyricinoleate in a highly filled suspension to its molecular properties. *LWT, 165*, Article 113704. https://doi.org/10.1016/j.lwt.2022.113704

Sereti, V., Kotsiou, K., Biliaderis, C. G., Moschakis, T., & Lazaridou, A. (2023). Development of oil-in-water emulsion gels enriched with barley β-glucan as potential solid fat substitute and evaluation of their physical properties. *Food Hydrocolloids, 145*, Article 109090. https://doi.org/10.1016/j.foodhyd.2023.109090

Sun, D., Wu, M., Bi, C., Gao, F., Wei, W., & Wang, Y. (2022). Using high-pressure homogenization as a potential method to pretreat soybean protein isolate: Effect on conformation changes and rheological properties of its acid-induced gel. *Innovative Food Science & Emerging Technologies, 82*, Article 103195. https://doi.org/10.1016/j.ifset.2022.103195

Tang, C., Wan, Z., Chen, Y., Tang, Y., Fan, W., Cao, Y., Song, M., Qin, J., Xiao, H., Guo, S., & Tang, Z. (2022). Structure and properties of organogels prepared from rapeseed oil with stigmasterol. *Foods, 11*, 939. https://doi.org/10.3390/foods11070939

Tao, C., Shkumatov, A. A., Alexander, S. T., Ason, B. L., & Zhou, M. (2019). Stigmasterol accumulation causes cardiac injury and promotes mortality. *Communications Biology, 2*, 20. https://doi.org/10.1038/s42003-018-0245-x

Wan, Z., Xia, H., Guo, S., & Zeng, C. (2021). Water-in-oil Pickering emulsions stabilized solely by a naturally occurring steroidal sapogenin: Diosgenin. *Food Research International, 147*, Article 110573. https://doi.org/10.1016/j.foodres.2021.110573

Wang, J., Huang, M., Yang, J., Ma, X., Zheng, S., Deng, S., Huang, Y., Yang, X., & Zhao, P. (2017). Anti-diabetic activity of stigmasterol from soybean oil by targeting the GLUT4 glucose transporter. *Food & Nutrition Research, 61*, 1364117. https://doi.org/10.1080/16546628.2017.1364117

Wang, J., Li, Y., Liu, H., & Tong, J. (2022). Surface tension, viscosity and electrical conductivity characteristics of new ether-functionalized ionic liquids. *Journal of Molecular Liquids, 351*, Article 118621. https://doi.org/10.1016/j.molliq.2022.118621

Wang, S., Yang, J., Shao, G., Qu, D., Zhao, H., Yang, L., Zhu, L., He, Y., Liu, H., & Zhu, D. (2020). Soy protein isolated-soy hull polysaccharides stabilized O/W emulsion: Effect of polysaccharides concentration on the storage stability and interfacial rheological properties. *Food Hydrocolloids, 101*. https://doi.org/10.1016/j.foodhyd.2019.105490. Article 105490.

Wijarnprecha, K., De Vries, A., Santiwattana, P., Sonwai, S., & Rousseau, D. (2019). Rheology and structure of oleogelled water-in-oil emulsions containing dispersed aqueous droplets as inactive fillers. *LWT, 115*, Article 108067. https://doi.org/10.1016/j.lwt.2019.04.068

Xia, W., Zhu, L., Delahaije, R. J., Cheng, Z., Zhou, X., & Sagis, L. M. (2022). Acid-induced gels from soy and whey protein thermally-induced mixed aggregates: Rheology and microstructure. *Food Hydrocolloids, 125*, Article 107376. https://doi.org/10.1016/j.foodhyd.2021.107376

Yang, Y., Fang, Z., Chen, X., Zhang, W., Xie, Y., Chen, Y., … Yuan, W. (2017). An overview of Pickering emulsions: Solid-particle materials, classification, morphology, and applications. *Frontiers in Pharmacology, 8*, 287. https://doi.org/10.3389/fphar.2017.00287

Yang, Y., Yu, P., Sun, J., Jia, Y., Wan, C., Zhou, Q., & Huang, F. (2022). Investigation of volatile thiol contributions to rapeseed oil by odor active value measurement and perceptual interactions. *Food Chemistry, 373*(B), Article 131607. https://doi.org/10.1016/j.foodchem.2021.131607

Zhang, Y., Zhou, F., Zeng, X., Shen, P., Yuan, D., Zhong, M., Zhao, Q., & Zhao, M. (2022). pH-driven-assembled soy peptide nanoparticles as particulate emulsifier for oil-in-water Pickering emulsion and their potential for encapsulation of vitamin D3. *Food Chemistry, 383*, Article 132489. https://doi.org/10.1016/j.foodchem.2022.132489

Zhi, L., Liu, Z., Wu, C., Ma, X., Hu, H., Liu, H., Adhikari, B., Wang, Q., & Shi, A. (2023). Advances in preparation and application of food-grade emulsion gels. *Food Chemistry, 424*, Article 136399. https://doi.org/10.1016/j.foodchem.2023.136399

Zhong, M., Xie, F., Zhang, S., Sun, Y., Qi, B., & Li, Y. (2020). Preparation and digestive characteristics of a novel soybean lipophilic protein-hydroxypropyl methylcellulose-calcium chloride thermosensitive emulsion gel. *Food Hydrocolloids, 106*, Article 105891. https://doi.org/10.1016/j.foodhyd.2020.105891